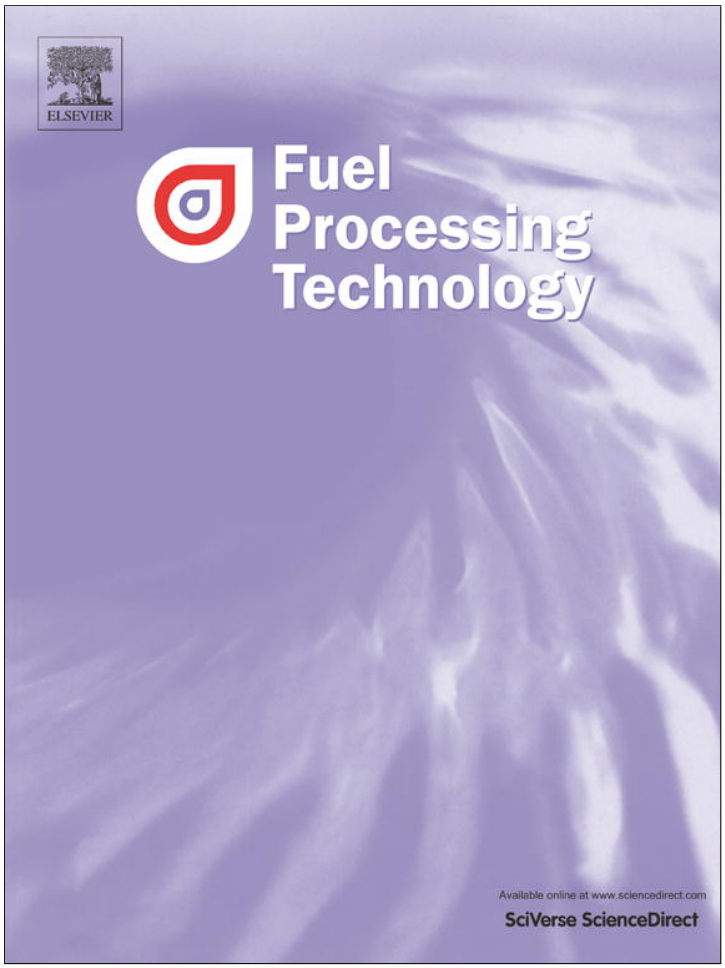

Fuel Processing Technology 112 (2013) 100–105

Contents lists available at SciVerse ScienceDirect

Fuel Processing Technology

journal homepage: www.elsevier.com/locate/fuproc

CO hydrogenation over Fe-promoted Rh–Mn–Li/SiO_2 catalyst: The effect of sequences for introducing the Fe promoter

Jun Yu [a,b], Dongsen Mao [a,*], Lupeng Han [a], Qiangsheng Guo [a], Guanzhong Lu [a,b]

[a] Research Institute of Applied Catalysis, School of Chemical and Environmental Engineering, Shanghai Institute of Technology, Shanghai 201418, PR China
[b] Key Lab for Advanced Materials and Research Institute of Industrial Catalysis, East China University of Science and Technology, Shanghai 200237, PR China

ARTICLE INFO

Article history:
Received 19 November 2012
Received in revised form 1 March 2013
Accepted 5 March 2013
Available online xxxx

Keywords:
Fe promoter
Impregnation sequence
Rh–Mn–Li/SiO_2
CO hydrogenation
C_2^+ oxygenates

ABSTRACT

The effects of different impregnation sequences for the precursors of iron and other metals (Rh, Mn, Li) on the catalytic properties of Fe-promoted Rh–Mn–Li/SiO_2 catalysts for the synthesis of C_2^+ oxygenates were investigated. The means of N_2 adsorption–desorption, XRD, H_2-TPR, in-situ FT-IR, and TPSR were used to characterize the physics-chemical properties of the catalysts. The results showed that when the iron was impregnated and calcined first followed by Rh–Mn–Li impregnation, it would availably inhibit the reduction of Rh and Mn oxides; however, if the iron was impregnated second onto a calcined Rh–Mn–Li/SiO_2 catalyst, it was more conducive to the dissociation and spillover of hydrogen, which could partly promote the reduction of Rh and Mn oxides. Based on the IR description and catalytic performance of the catalysts for CO hydrogenation, it is conceivable that the facile transformation of dicarbonyl $Rh^+(CO)_2$ into H–Rh–CO and Rh–CO–Fe is responsible for the higher selectivity of C_2^+ oxygenates over the catalyst, in which Fe was impregnated and calcined first followed by Rh–Mn–Li impregnation.

1. Introduction

Oxygenated compounds with two or more carbon atoms (e.g. ethanol, acetaldehyde, acetic acid) are important raw chemicals and, among other possibilities, can be used as fuel additives [1]. Thus, developing new types of catalysts to synthesize these oxygenated compounds from synthesis gas, which can be conveniently manufactured from natural gas, coal and biomass, is very meaningful for societal development because of the global demand for the decrease in the dependence on petroleum [2,3]. Many catalysts, particularly Rh-, Co-, Cu- and Mo-based catalysts, have been reported to be capable of catalytic transformation of syngas to ethanol and other C_2^+ oxygenates [4,5]. However, most of the catalysts still suffer from low productivity and oxygenated compound selectivity.

Under the tireless efforts, silica supported rhodium based catalysts are found to be the most promising catalysts because of their exceptionally high selectivity towards oxygenated products [6–10]. Moreover, the addition of appropriate promoters can further enhance the rate of formation of oxygenates, especially ethanol [11–17]. Thus, understanding of the functioning mechanism of the promoter should be helpful for the rational design of efficient catalysts for the synthesis of C_2^+ oxygenates during CO hydrogenation. As one part of the functioning mechanism, it has been mentioned that the right position of promoters in the catalyst is quite important for obtaining better catalytic performances [18–20]. For instance, Ledford et al. [21] studied two methods of preparing La^{3+}-promoted Co/Al_2O_3 catalysts. They noted promotional effect only when La^{3+} was impregnated and calcined first followed by Co impregnation. Nevertheless, no effect was observed when La^{3+} was impregnated second onto a calcined Co/Al_2O_3 catalyst.

On the other hand, many studies have demonstrated that small quantities of iron promoted the activity for CO hydrogenation on Rh-based/SiO_2 catalysts, and affected the selectivity, such as increasing the production of ethanol at the expense of acetaldehyde and acetic acid [22,23]. In our previous study, we have also found that the catalytic performance of Rh–Mn–Li/SiO_2 catalyst for the synthesis of C_2^+ oxygenates from CO hydrogenation was enhanced by Fe doping [24]. However, most of the research merely focused on the influence of iron content, and few studies about the effect of preparation methods for introducing the Fe promoter have been investigated before. To the best of our knowledge, only Wang et al. [25] have briefly reported that the catalyst prepared by the impregnation of a FeO_x–SiO_2 composite with $Rh(NO_3)_3$ aqueous solution provided better ethanol formation activity than those prepared by co-impregnation method, but no more detailed reports have been followed so far. Inspired by the La^{3+}-promoted Co/Al_2O_3 catalysts mentioned above, it is conceivable that the further study of the effect of the impregnation sequences of Fe and Rh on CO hydrogenation should be helpful for the better understanding of the Rh–Fe interaction and design of the catalysts.

This study is followed by our previous study, which has investigated the effect of the amount of iron promoter on the catalytic properties of Rh–Mn–Li/SiO_2 catalyst in CO hydrogenation [24]. In this paper, we prepared the Fe-promoted Rh–Mn–Li/SiO_2 catalyst by three different

* Corresponding author. Tel.: +86 21 6087 7221; fax: +86 21 6087 7231.
E-mail address: dsmao1106@yahoo.com.cn (D. Mao).

0378-3820/$ – see front matter © 2013 Elsevier B.V. All rights reserved.
http://dx.doi.org/10.1016/j.fuproc.2013.03.004

methods: 1) Fe was impregnated and calcined first followed by Rh–Mn–Li impregnation; 2) all the precursors of metals were co-impregnated; 3) Fe was impregnated second onto a calcined Rh–Mn–Li/SiO_2 catalyst. The main novel contribution of this work is the study of how the catalytic activity and selectivity are affected by the different position of Fe in the Rh–Mn–Li/SiO_2 catalyst.

2. Experimental

2.1. Catalyst preparation

SiO_2 was prepared by the modified Stöber method [26]. In a typical synthesis, solution I was prepared by mixing 21 mL TEOS (99.5%, SCRC) with 50 mL anhydrous ethanol (99.7%, SCRC); solution II was composed of 76 mL $NH_3 \cdot H_2O$ (26 vol.%, SCRC) and 200 mL anhydrous ethanol. Secondly, solution I was added slowly into solution II in a flask under rapid stirring at 25 °C and reacted for 4 h. The white solid product was recovered by centrifugation (7000 rpm), which was washed with absolute ethanol for three times and dried at 90 °C. Before used, it was calcined in static air at 350 °C for 4 h.

$RhCl_3$ hydrate (Rh ~36 wt.%, Fluka), $Mn(NO_3)_2 \cdot 6H_2O$ (99.99%, SCRC), $Fe(NO_3)_3 \cdot 6H_2O$ (99.99%, SCRC), and Li_2CO_3 (99.5%, SCRC) were used in catalyst preparations. Co-impregnation and sequential impregnation methods were employed for the preparation of Fe-promoted Rh–Mn–Li catalysts supported on SiO_2 (Rh loading was 1.5 wt.% based on the weight of SiO_2, and the weight ratio of Fe:Rh:Mn:Li = 0.1:1.5:1.5:0.07). For the catalyst referred to as RMLFe/SiO_2 prepared by the co-impregnation method, the SiO_2 was added into the aqueous solution of $RhCl_3$ hydrate and other promoter precursors, followed by drying at 90 °C for 4 h and then at 120 °C overnight before being calcined in air at 350 °C for 4 h. For the sequential impregnation method, the SiO_2 was impregnated with the aqueous solution of $Fe(NO_3)_3$ and mixed aqueous solution containing $RhCl_3$ hydrate, $Mn(NO_3)_2$ and Li_2CO_3 by different impregnation sequences. More detailed, Fe was impregnated and calcined first followed by Rh–Mn–Li impregnation over RML/Fe/SiO_2 catalyst; and Fe was impregnated second onto a calcined Rh–Mn–Li/SiO_2, which was noted as Fe/RML/SiO_2. For comparison purpose, the sample referred to as Fe/SiO_2 or RML/SiO_2 in the text was impregnated with either the aqueous solution of $Fe(NO_3)_3$ or the mixed aqueous solution containing $RhCl_3$ hydrate, $Mn(NO_3)_2$ and Li_2CO_3, the contents of the metals were consistent with the above catalysts.

2.2. CO hydrogenation

CO hydrogenation was performed in a fixed-bed micro-reactor with length ~350 mm and internal diameter ~5 mm. The micro-reactor was made of stainless steel. According to the activity result of preliminary experiment, it indicated that there were no products produced without the participation of catalysts. The catalyst (0.3 g) was diluted with inert α-alumina (1.2 g) to avoid channeling and hot spots. Prior to reaction, the catalyst was heated to 400 °C (heating rate ~3 °C/min) and reduced with H_2/N_2 (molar ratio of H_2/N_2 = 1/9, total flow rate = 50 mL/min) for 2 h at atmospheric pressure. The catalyst was then cooled down to 300 °C and the reaction started as gas flow was switched to a H_2/CO mixture (molar ratio of H_2/CO = 2, total flow rate = 50 mL/min (STP)) at 3 MPa. All post-reactor lines and valves were heated to 150 °C to prevent product condensation. The products were analyzed on-line (Agilent GC 6820) using a HP-PLOT/Q column (30 m, 0.32 mm ID) with an FID (flame ionization detector) and a TDX-01 column with a TCD (thermal conductivity detector). The CO conversion was calculated based on the fraction of CO that formed carbon-containing products and the selectivity of a certain product was calculated based on carbon efficiency, as reported previously [27,28].

2.3. Catalyst characterization

NH_3 temperature programmed desorption (NH_3-TPD) was carried out in a quartz microreactor. The sample (0.05 g) was pretreated at 500 °C for 1 h under a N_2 flow (50 mL/min). After the temperature decreased to 30 °C, NH_3 was introduced for adsorbing on the surface, followed by evacuation at 100 °C for 1 h to eliminate the weakly physical adsorbed species. Then, the temperature was ramped from 100 °C to 550 °C at 10 °C/min while the effluent gas was analyzed with a TCD.

H_2 temperature-programmed reduction (TPR) was carried out in a quartz microreactor. 0.1 g of the as-prepared sample was first pretreated at 350 °C in O_2/N_2 (molar ratio of O_2/N_2 = 1/4) for 1 h prior to a TPR measurement. During the TPR experiment, H_2/N_2 (molar ratio of H_2/N_2 = 1/9) was used at 50 mL/min and the temperature was ramped from room temperature to 500 °C at 10 °C/min while the effluent gas was analyzed with a TCD.

CO adsorption was studied using a Nicolet 6700 FT-IR spectrometer equipped with a DRIFT (diffuse reflectance infrared Fourier transform) cell with CaF_2 windows. The sample in the cell was pretreated in H_2/N_2 (molar ratio of H_2/N_2 = 1/9) at 400 °C for 2 h, and then the temperature was dropped to room temperature. After the cell was outgassed in vacuum to $<10^{-3}$ Pa, the background was recorded. After CO was introduced for 80 min ($p_{co} = 8.0 \times 10^3$ Pa), the IR spectrum of CO adsorbed on the catalyst was recorded. Then the mixture of H_2/N_2 was introduced again, and the IR spectrum of adsorbed CO was recorded as a function of time. The concentration of CO was higher than 99.97%, and it was pretreated by dehydration and deoxygenization before being used. The spectral resolution was 4 cm^{-1} and the number of scans was 64.

The temperature-programmed surface reaction (TPSR) experiments were carried out as follows: after the catalyst was reduced at 400 °C in H_2/N_2 (molar ratio of H_2/N_2 = 1/9) for 2 h, it was cooled down to room temperature and CO was introduced for adsorption for 0.5 h; afterwards, the H_2/N_2 mixture was swept again, and the temperature was increased at the rate of 10 °C/min with a quadrupole mass spectrometer (QMS, Balzers OmniStar 200) as the detector to monitor the signal of CH_4 (m/z = 15).

3. Results and discussion

3.1. CO hydrogenation results

The effects of different impregnation sequences for the precursors of iron and other metals on the catalytic properties of Rh–Mn–Li–Fe/SiO_2 catalysts in CO hydrogenation are shown in Table 1. For comparison, the catalytic properties of single Fe-supported SiO_2 (Fe/SiO_2) and RML/SiO_2 are also included in the table. As shown, CO_2 and hydrocarbons were the principal products over the 0.1Fe/SiO_2 catalyst, with a selectivity of 22.1% and 72.1%, respectively; and only a little C_2^+ oxygenates were detected, with a selectivity of 4.8%. Compared with the Fe/SiO_2 catalyst, the RML/SiO_2 catalyst showed better catalytic properties for the synthesis of C_2^+ oxygenates, and the promotion of Fe could further enhance the activity of RML/SiO_2 catalyst. Moreover, it can be seen that the activity over the Fe promoted catalysts under the same conditions decreased in a sequence: RML/Fe/SiO_2 ≈ RMLFe/SiO_2 > Fe/RML/SiO_2. With respect to product selectivity, the highest C_2^+ oxygenates selectivity along with the lowest C_2^+ hydrocarbons selectivity was obtained on RML/Fe/SiO_2 catalyst. The formation of the undesirable by-product CH_4 and CO_2 were similar on RML/Fe/SiO_2 and RMLFe/SiO_2 catalysts, which were much lower than that on Fe/RML/SiO_2 catalyst. Furthermore, it is noteworthy that the yield of the C_2^+ oxygenates increased remarkably from 266.2 g/(kg·h) over Fe/RML/SiO_2 to 562.8 g/(kg·h) over RML/Fe/SiO_2. These results suggest that the sequence of Fe addition significantly

Table 1
Catalytic properties for CO hydrogenation on different Rh–Mn–Li–Fe/SiO_2 catalysts.

Catalyst	CO conv. (C%)	Selectivity of products (C%)							STY(C_2^+ Oxy)[c] (g/(kg · h))
		CO_2	CH_4	MeOH	AcH	EtOH	C_2^+ Oxy[a]	C_2^+ HC[b]	
Fe/SiO_2	9.3	22.1	7.2	1.0	1.0	2.0	4.8	64.9	15.6
RML/SiO_2	18.9	1.1	12.1	2.3	25.4	27.1	54.3	30.2	309.1
RML/Fe/SiO_2	28.5	1.1	11.8	0.5	30.6	32.7	64.3	22.3	562.8
RMLFe/SiO_2	28.2	1.4	11.7	0.6	32.8	22.9	58.2	28.1	491.0
Fe/RML/SiO_2	19.7	3.8	17.7	1.1	28.1	16.5	45.6	31.8	266.2

Reaction conditions: 300 °C, 3 MPa, *S.V.* = 10,000 mL/(g·h), $V(H_2)$ / $V(CO)$ = 2, data taken after 15 h when steady state reached. Experimental error: ±5%.
[a] C_2^+ Oxy denotes oxygenates containing two and more carbon atoms.
[b] C_2^+ HC denotes hydrocarbons containing two and more carbon atoms.
[c] STY(C_2^+ Oxy): space time yield of C_2^+ Oxy.

affect the activity and product selectivity over the RML/SiO_2 catalyst in CO hydrogenation.

3.2. Structural and textural characterization

Firstly, the samples were characterized by XRD and N_2 adsorption–desorption. XRD patterns (not shown) of the support and corresponding catalysts showed no crystalline phases, indicating that the SiO_2 is XRD-amorphous and the metal particles are highly dispersed. The similar BET surface areas (~15 m^2/g) were obtained on all the samples.

On the basis of the above results, it is not surprising that the different impregnation sequences cannot influence the high dispersion of Rh and other promoters since the loadings of Rh and promoters were relatively low, and this can also explain why no significant difference was observed in the BET surface areas of the different catalysts.

3.3. NH_3-TPD

NH_3-TPD was used as a tool for measuring the changes of surface acidity depending on the methodology of iron incorporation. All the catalysts did not show a noticeable peak in the NH_3-TPD profiles (not shown here), indicating that there is almost no acid site on the surface of all the catalysts investigated in the work.

Based on the result, it is conceivable that whether the support of SiO_2 or the loaded metals showed no acidity, and the methodology of iron incorporation cannot influence the surface acidity of the Fe-promoted Rh–Mn–Li/SiO_2 catalysts. Thus, it is inferred that the change of catalytic activities over the Fe-promoted Rh–Mn–Li/SiO_2 catalysts is not related to the surface acidity of catalysts.

3.4. H_2-TPR

Fig. 1 shows the temperature programmed reduction (TPR) profiles for all the catalysts. For comparison, the profiles of single Fe-supported SiO_2 (Fe/SiO_2) and RML/SiO_2 are also included in the figure. It can be seen that no evident reduction peak appeared on the only Fe-supported SiO_2 sample, implying that the amount of Fe (0.1 wt.%) was too small to be detected. As reported in previous paper [24], there were three peaks of H_2 consumption in the TPR profile of RML/SiO_2 catalyst. The high temperature peak centered around 300 °C was ascribed to the reduction of MnO_2 [29,30], and the major peak at 135 °C and the shoulder peak at 157 °C were assigned to the reduction of Rh_2O_3 not intimately contacting with Mn species (denoted as Rh(I)) and of Rh_2O_3 intimately contacting with Mn species (denoted as Rh(II)), respectively [22,30].

It is evident that the different impregnation sequences for the iron and other metals remarkably affected the reducibility of Rh and Mn oxides. Compared with the catalyst of RML/SiO_2, the reduction peaks of Rh(I) and Rh(II) over RML/Fe/SiO_2 catalyst shifted to the higher temperatures (140 °C and 167 °C), while the amount of Rh(II) greatly increased along with a decrease of the amount of Rh(I). At the same time, the reduction peak of MnO_2 diminished along with a slight shift to a higher reduction temperature (305 °C). It is suggested that when the iron layer in the Rh and Mn below, the iron would availably inhibit the reduction of Rh and Mn oxides. In the related works, the inhibition of Rh reduction in the presence of iron oxide was also proved by Burch et al. [12] and Mo et al. [15]. As the iron was impregnated from inner layer to outside of the catalyst, the reduction peaks of Rh and Mn would slightly shift to the lower temperatures again, and the two reduction peaks of Rh oxides incorporated gradually. It is conceivable that the effect of Fe on the inhibition of Rh and Mn reduction can be weakened when the iron was impregnated from inner layer to outside of the catalyst.

The TPR results showed clearly that different interaction among Rh, Mn and Fe occurred when the impregnation sequences changed. It is concluded that the Fe species achieved closer contacts with the Rh and Mn species as the Fe layer in the Rh and Mn below. This closer interaction could lead to an increase in the Rh–Fe interface, where the C atom of the adsorbed CO is thought to be attached to the Rh atom, while the O atom to the Fe ion [12]. This mode of CO adsorption is thought to be the most vital in the catalytic synthesis of oxygenates from CO hydrogenation [13]. Thus, enhancement in the selectivity of C_2^+ oxygenates, especially in the selectivity of ethanol, can be explained in terms of the two-site activation of tilted adsorbed CO with Rh–Fe species, which is also consistent with our FT-IR result showed as below.

3.5. FT-IR

A series of infrared spectra of the in situ reduced catalysts after CO adsorption at 30 °C for 80 min are compared in Fig. 2. It can be seen that the IR spectra of the adsorbed CO all exhibited a band around 2067 cm^{-1} and a doublet at 2104 and 2034 cm^{-1} with different relative intensities. The 2067 cm^{-1} band can be attributed to the linear

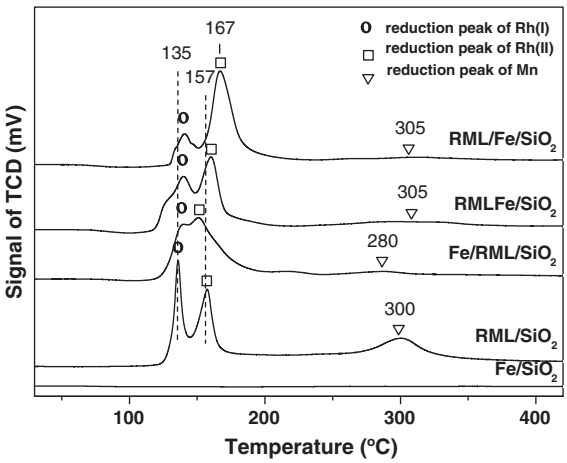

Fig. 1. The TPR profiles of the different catalysts.

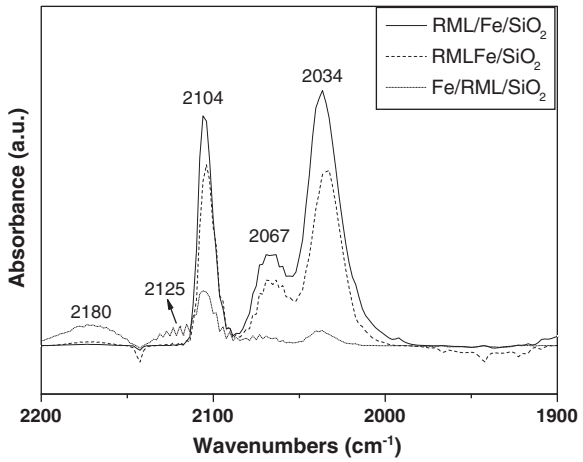

Fig. 2. The infrared spectra after CO adsorption on the different catalysts at 30 °C for 80 min.

adsorbed CO [CO(l)] and the doublet can be assigned to the symmetric and asymmetric carbonyl stretching of the dicarbonyl $Rh^{+}(CO)_2$ [CO(gdc)] [31]. It is widely accepted that the dicarbonyl species can only be formed on the Rh^{+} sites which may be highly dispersed and linear CO on the Rh^{0} sites [32,33]. As the addition of iron was gradually impregnated from inner layer to outside, the intensities of adsorbed CO species decreased. Meanwhile, the bands centered at around 2180 and 2125 cm^{-1}, which can be attributed to gaseous CO [34], increased.

Based on the above results, it is conceivable that the position of Fe can influence the CO adsorption considerably, considering that the total CO adsorption of $Fe/RML/SiO_2$ catalyst decreased remarkably due to the decrease of Rh coverage compared to that of $RML/Fe/SiO_2$ catalyst.

Fig. 3 shows the IR spectra of adsorbed species on the in situ reduced catalysts by H_2/N_2 flow flushed into the cell after CO adsorbed at 30 °C. As observed, the CO(l) band on $RML/Fe/SiO_2$ catalyst decreased rapidly at first. As the time increases, the intensity of CO(gdc) decreased, along with the new bands at around 2055 cm^{-1} and 1990 cm^{-1} raising slowly. The 2055 cm^{-1} band can be attributed to rhodium carbonyl hydride species [H–Rh–CO] (i.e., re-formation of metallic Rh from isolated Rh^{+}) [35–37]. Considering the fact that band at 1990 cm^{-1} is intermediate between the Rh–CO and Fe–CO [38] stretching frequencies, it can be assigned to the Rh–CO–Fe species, as has been proposed by Guglielminotti et al. [23]. For the $Fe/RML/SiO_2$ catalyst, it can be seen differently that the adsorbed CO decreased as a function of time, and no new bands appeared. Although the spectra for the desorption behavior of adsorbed CO on $RMLFe/SiO_2$ catalyst were similar to that on $RML/Fe/SiO_2$, it is obvious that the transformation ability of CO(gdc) into H–Rh–CO or Rh–CO–Fe species was weaker, and more adsorbed CO was desorbed compared to that of $RML/Fe/SiO_2$.

Based on the above IR results, it is suggested that the CO(gdc) species can be changed in two different modes: (a) desorbed associatively, (b) transformed into H–Rh–CO or Rh–CO–Fe species, and the different positions of iron in the catalysts resulted in remarkable changes in desorption/transformation behavior of adsorbed CO in the presence of hydrogen. The CO(gdc) species on $RML/Fe/SiO_2$ catalyst can be easily transformed to H–Rh–CO and Rh–CO–Fe species; however, the CO(gdc) species on $Fe/RML/SiO_2$ catalyst only desorbed in the H_2 atmosphere. By combining the catalytic properties of the catalysts and above discussions, it can be inferred that the catalytic performances of the catalysts are related to the desorption/transformation behavior of CO(gdc) species in the reaction, and the facile transformation of CO(gdc) into H–Rh–CO and Rh–CO–Fe is responsible for high

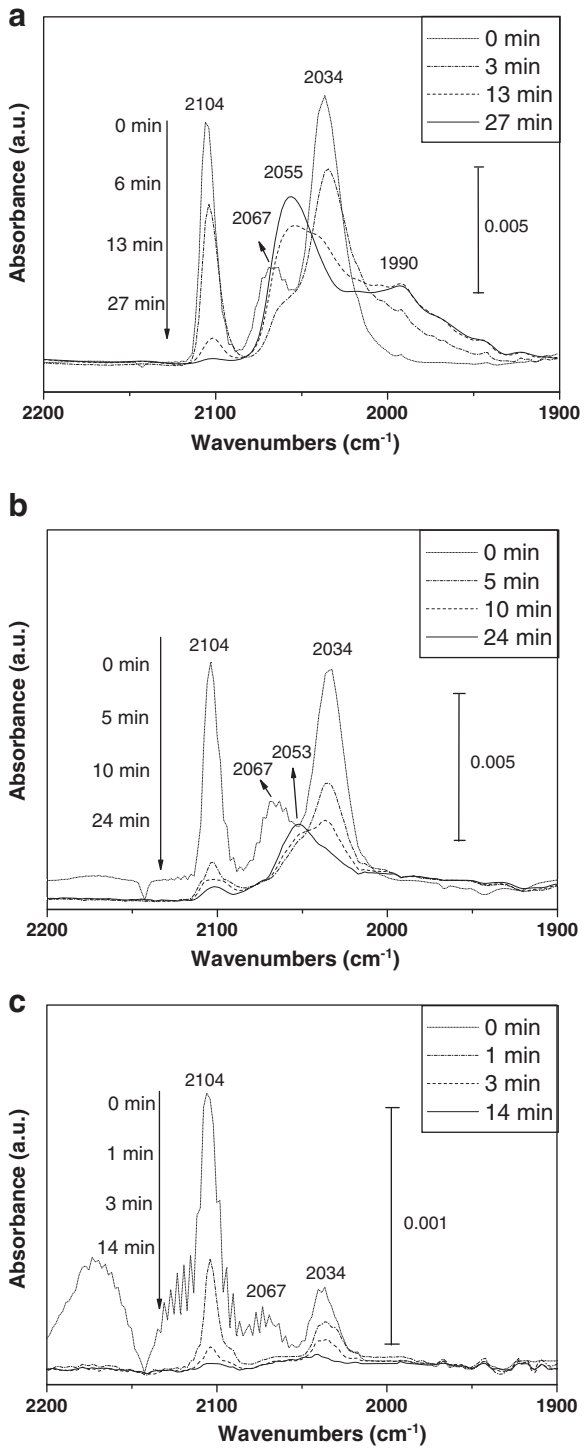

Fig. 3. The infrared spectra after CO adsorption at 30 °C for 80 min followed by flushing with 10% H_2/N_2 (time = 0, start of H_2/N_2 flushing) on different catalysts: a) $RML/Fe/SiO_2$, b) $RMLFe/SiO_2$, c) $Fe/RML/SiO_2$.

selectivity of C_2^{+} oxygenates, which is consistent with our previous conclusion [24] and proposition by Guglielminotti et al. [23].

3.6. TPSR result

Since the hydrogenation of dissociated CO into CH_4 is very fast on the Rh-based catalyst, the methane formation in TPSR can be used as a tool for measuring the CO dissociation over such catalysts [39]. Fig. 4 shows the profiles of CH_4 production on the catalysts. It can be seen that on the profile of $RMLFe/SiO_2$ catalyst, the peak of CH_4 formation

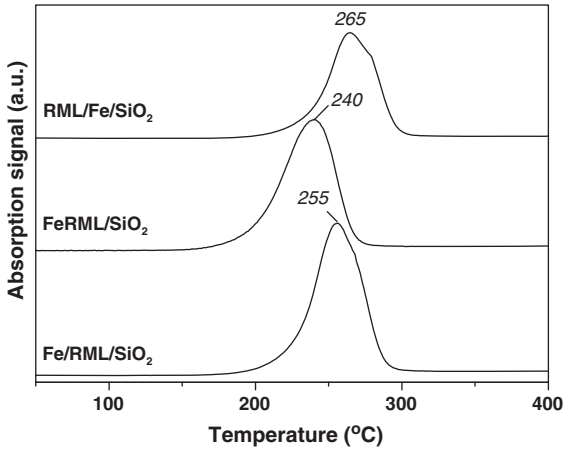

Fig. 4. The TPSR profiles of the different catalysts.

was centered at around 240 °C; however, the CH_4 peak shifted to 255 °C and 265 °C on $Fe/RML/SiO_2$ and $RML/Fe/SiO_2$, respectively, implying that weaker CO dissociation ability was obtained on them. In addition, the amounts of CH_4 produced by the catalysts were different: the amount of CH_4 produced on the $Fe/RML/SiO_2$ was the largest among the three catalysts; whereas on $RML/Fe/SiO_2$, the intensity of CH_4 peak was much lower than that on the other two catalysts. According to the viewpoint of Yuan and co-workers [40], this observation indicates that the number of active sites responsible for methane production decreased in the following order: $Fe/RML/SiO_2 > RMLFe/SiO_2 > RML/Fe/SiO_2$.

CO dissociation is believed to be the first step in the synthesis of C_2^+ oxygenates, and the resulting surface carbon is then hydrogenated to form a surface hydrocarbon species, $(CH_x)_{ads}$. This $(CH_x)_{ads}$ species can then undergo: (a) hydrogenation to form methane, or (b) CO insertion to form oxygenates, or (c) chain growth to form higher hydrocarbons. The hydrogenation to form methane and the formation of oxygenates from CO insertion are the couple of competitive routes to the reaction. Thus, considering that the iron in the catalyst surface was more favorable for hydrogenation, the higher selectivity of CH_4 was obtained over $Fe/RML/SiO_2$ catalyst.

4. Conclusions

The effects of different impregnation sequences for the precursors of iron and other metals on the catalytic properties of Fe-promoted $Rh–Mn–Li/SiO_2$ catalysts for the synthesis of C_2^+ oxygenates were investigated. The results showed that the different positions of Fe in the catalyst markedly influenced the catalytic performance of the catalysts. The highest CO conversion and yield of C_2^+ oxygenates were obtained on the $RML/Fe/SiO_2$, in which Fe was impregnated and calcined first followed by Rh–Mn–Li impregnation.

The H_2–TPR result showed that the different impregnation sequences for the precursors of iron and other metals remarkably affected the reducibility of Rh and Mn oxides. It is suggested that when the iron layer in the Rh and Mn below, the iron would availably inhibit the reduction of Rh and Mn oxides; however, the iron in the catalyst surface was more conducive to the dissociation and spillover of hydrogen, which could partly promote the reduction of Rh and Mn oxides. The result of TPSR also suggested that the iron in the catalyst surface was more favorable for hydrogenation, resulting in the higher selectivity of CH_4 over the catalyst of $Fe/RML/SiO_2$. Based on the IR description and the catalytic performance of the catalysts for CO hydrogenation, it is conceivable that the facile transformation of CO(gdc) into H–Rh–CO and Rh–CO–Fe is responsible for the higher selectivity of C_2^+ oxygenates, especially for ethanol, over $RML/Fe/SiO_2$ catalyst.

Acknowledgments

The authors gratefully acknowledge financial support from the Science and Technology Commission of Shanghai Municipality (08520513600), Leading Academic Discipline Project of Shanghai Education Committee (J51503) and Shanghai Institute of Technology (KJ2011-02).

References

[1] G.A. Mills, Status and future opportunities for conversion of synthesis gas to liquid fuels, Fuel 73 (1994) 1243–1279.
[2] A.Y. Khodakov, W. Chu, P. Fongarland, Advances in the development of novel cobalt Fischer–Tropsch catalysts for synthesis of long-chain hydrocarbons and clean fuels, Chemical Reviews 107 (2007) 1692–1744.
[3] Q.H. Zhang, J.C. Kang, Y. Wang, Development of novel catalysts for Fischer–Tropsch synthesis: tuning the product selectivity, ChemCatChem 2 (2010) 1030–1058.
[4] J.J. Spivey, A. Egbebi, Heterogeneous catalytic synthesis of ethanol from biomass-derived syngas, Chemical Society Reviews 36 (2007) 1514–1528.
[5] V. Subramani, S.K. Gangwal, A review of recent literature to search for an efficient catalytic process for the conversion of syngas to ethanol, Energy & Fuels 22 (2008) 814–839.
[6] M.A. Haider, M.R. Gogate, R.J. Davis, Fe-promotion of supported Rh catalysts for direct conversion of syngas to ethanol, Journal of Catalysis 261 (2009) 9–16.
[7] S.S.C. Chuang, R.W. Stevens Jr., R. Khatri, Mechanism of C_{2+} oxygenate synthesis on Rh catalysts, Topics in Catalysis 32 (2005) 225–232.
[8] J.P. Hindermann, G.J. Hutchings, A. Kiennemann, Mechanistic aspects of the formation of hydrocarbons and alcohols from CO hydrogenation, Catalysis Reviews — Science and Engineering 35 (1993) 1–127.
[9] G. Van der Lee, V. Ponec, On some problems of selectivity in syngas reactions on the group VIII metals, Catalysis Reviews — Science and Engineering 29 (1987) 183–218.
[10] H. Arakawa, T. Fukushima, M. Ichikawa, Selective synthesis of ethanol over Rh–Ti–Fe–Ir/SiO_2 catalyst at high pressure syngas conversion, Chemistry Letters 163 (1985) 881–884.
[11] M.M. Bhasin, W.J. Bartley, P.C. Ellgen, T.P. Wilson, Synthesis gas conversion over supported rhodium and rhodium–iron catalysts, Journal of Catalysis 54 (1978) 120–128.
[12] R. Burch, M.J. Hayes, The preparation and characterization of Fe-promoted Al_2O_3-supported Rh catalysts for the selective production of ethanol from syngas, Journal of Catalysis 165 (1997) 249–263.
[13] W.M. Chen, Y.J. Ding, X.G. Song, T. Wang, H.Y. Luo, Promotion effect of support calcination on ethanol production from CO hydrogenation over Rh/Fe/Al_2O_3 catalysts, Applied Catalysis A: General 407 (2011) 231–237.
[14] J. Gao, X. Mo, A.C. Chien, W. Torres, J.G. Goodwin Jr., CO hydrogenation on lanthana and vanadia doubly promoted Rh/SiO_2 catalysts, Journal of Catalysis 262 (2009) 119–126.
[15] X. Mo, J. Gao, N. Umnajkaseam, J.G. Goodwin Jr., La, V, and Fe promotion of Rh/SiO_2 for CO hydrogenation: effect on adsorption and reaction, Journal of Catalysis 267 (2009) 167–176.
[16] D. Mei, R. Rousseau, S.M. Kathmann, V.A. Glezakou, M.H. Engelhard, W. Jiang, C. Wang, M.A. Gerber, J.F. White, D.J. Stevens, Ethanol synthesis from syngas over Rh-based/SiO_2 catalysts: a combined experimental and theoretical modeling study, Journal of Catalysis 271 (2010) 325–342.
[17] N.D. Subramanian, J. Gao, X. Mo, J.G. Goodwin Jr., W. Torres, J.J. Spivey, La and/or V oxide promoted Rh/SiO_2 catalysts: effect of temperature, H_2/CO ratio, space velocity, and pressure on ethanol selectivity from syngas, Journal of Catalysis 272 (2010) 204–209.
[18] R. Burch, M.I. Petch, Investigation of the synthesis of oxygenates from carbon monoxide/hydrogen mixtures on supported rhodium catalysts, Applied Catalysis A: General 88 (1992) 39–60.
[19] M. Ichikawa, T. Fukushima, EXAFS evidence for direct rhodium–iron bonding in silica-supported rhodium–iron bimetallic catalysts, The Journal of Physical Chemistry 90 (1986) 1222–1224.
[20] M.R. Gogate, R.J. Davis, X-ray absorption spectroscopy of an Fe-promoted Rh/TiO_2 catalyst for synthesis of ethanol from synthesis gas, ChemCatChem 1 (2009) 295–303.
[21] J.S. Ledford, M. Houalla, A. Proctor, D.M. Hercules, L. Petrakis, Influence of lanthanum on the surface structure and carbon monoxide hydrogenation activity of supported cobalt catalysts, The Journal of Physical Chemistry 93 (1989) 6770–6777.
[22] H.M. Yin, Y.J. Ding, H.Y. Luo, H.J. Zhu, D.P. He, J.M. Xiong, L.W. Lin, Influence of iron promoter on catalytic properties of Rh–Mn–Li/SiO_2 for CO hydrogenation, Applied Catalysis A: General 243 (2003) 155–164.
[23] E. Guglielminotti, F. Pinna, M. Rigoni, G. Strukul, L. Zanderighi, The effect of iron on the activity and the selectivity of Rh/ZrO_2 catalysts in the CO hydrogenation, Journal of Molecular Catalysis A: Chemical 103 (1995) 105–116.
[24] J. Yu, D.S. Mao, L.P. Han, Q.S. Guo, G.Z. Lu, The effect of Fe on the catalytic performance of Rh–Mn–Li/SiO_2 catalyst: a DRIFTS study, Catalysis Communications 27 (2012) 1–4.
[25] J.J. Wang, Q.H. Zhang, Y. Wang, Rh-catalyzed syngas conversion to ethanol: studies on the promoting effect of FeO_x, Catalysis Today 171 (2011) 257–265.
[26] M. Szekeres, O. Kamalin, P.G. Grobet, R.A. Schoonheydt, K. Wostyn, K. Clays, A. Persoons, I. Dkénáy, Two-dimensional ordering of Stöber silica particles at the

air/water interface, Colloids and Surfaces A: Physicochemical and Engineering Aspects 227 (2003) 77–83.
[27] J. Yu, D.S. Mao, L.P. Han, Q.S. Guo, G.Z. Lu, Enhanced C_2 oxygenate synthesis by CO hydrogenation over Rh-based catalyst supported on a novel SiO_2, Catalysis Communications 24 (2012) 25–29.
[28] L.P. Han, D.S. Mao, J. Yu, Q.S. Guo, G.Z. Lu, Synthesis of C_2-oxygenates from syngas over Rh-based catalyst supported on SiO_2, TiO_2 and SiO_2–TiO_2 mixed oxide, Catalysis Communications 23 (2012) 20–24.
[29] H.Y. Luo, P.Z. Lin, S.B. Xie, H.W. Zhou, C.H. Xu, S.Y. Huang, L.W. Lin, D.B. Liang, P.L. Yin, Q. Xin, The role of Mn and Li promoters in supported rhodium catalysts in the formation of acetic acid and acetaldehyde, Journal of Molecular Catalysis A: Chemical 122 (1997) 115–123.
[30] D.H. Jiang, Y.J. Ding, Z.D. Pan, X.M. Li, G.P. Jiao, J.W. Li, W.M. Chen, H.Y. Luo, Roles of chlorine in the CO hydrogenation to C_2-oxygenates over Rh–Mn–Li/SiO_2 catalysts, Applied Catalysis A: General 331 (2007) 70–77.
[31] S.D. Worley, G.A. Mattson, R. Caudlll, An infrared study of the hydrogenation of CO on supported Rh catalysts, The Journal of Physical Chemistry 87 (1983) 1671–1673.
[32] R.R. Cavanagh, J.T. Yates Jr., Site distribution studies of Rh supported on Al_2O_3—an infrared study of chemisorbed CO, The Journal of Chemical Physics 74 (1981) 4150–4155.
[33] C.A. Rice, S.D. Worley, C.W. Curtis, J.A. Guin, A.R. Tarrer, The oxidation state of dispersed Rh on Al_2O_3, The Journal of Chemical Physics 74 (1981) 6487–6497.
[34] X. Mo, J. Gao, J.G. Goodwin Jr., Role of promoters on Rh/SiO_2 in CO hydrogenation: a comparison using DRIFTS, Catalysis Today 147 (2009) 139–149.
[35] F. Solymosi, M. Pásztor, Infrared study of the effect of H_2 on CO-induced structural changes in supported Rh, The Journal of Physical Chemistry 90 (1986) 5312–5317.
[36] F. Solymosi, A. Erdöhelyi, M. Kocsis, Surface interaction between H_2 and CO_2 on $RhAl_2O_3$, studied by adsorption and infrared spectroscopic measurements, Journal of Catalysis 65 (1980) 428–436.
[37] M.L. McKee, C.H. Dai, S.D. Worley, The rhodium carbonyl hydride species. A theoretical and experimental investigation, The Journal of Physical Chemistry 92 (1988) 1056–1059.
[38] U. Seip, M.C. Tsai, K. Christmann, J. Kuppers, G. Ertl, Interaction of Co with an Fe(111) surface, Surface Science 139 (1984) 29–42.
[39] M. Ojeda, M.L. Granados, S. Rojas, P. Terreros, F.J. García-García, J.L.G. Fierro, Manganese-promoted Rh/Al_2O_3 for C_2-oxygenates synthesis from syngas: effect of manganese loading, Applied Catalysis A: General 261 (2004) 47–55.
[40] G.C. Chen, C.Y. Guo, X.H. Zhang, Z.J. Huang, G.Q. Yuan, Direct conversion of syngas to ethanol over Rh/Mn-supported on modified SBA-15 molecular sieves: effect of supports, Fuel Processing Technology 92 (2011) 456–461.